Journal of Structural Geology, Vol. 15, No. 8, pp. 983 to 993, 1993
Printed in Great Britain

0191-8141/93 $06.00+0.00

Structural analysis of sheath folds in the Sylacauga Marble Group, Talladega slate belt, southern Appalachians

JONATHAN W. MIES

Geological Survey of Alabama, P.O. Box O, Tuscaloosa, AL 35486-9780, U.S.A.

(*Received* 31 *March* 1992; *accepted in revised form* 20 *October* 1992)

Abstract—Remnant blocks of marble from the Moretti-Harrah dimension-stone quarry provide excellent exposure of meter-scale sheath folds. Tubular structures with elliptical cross-sections ($4 \leq R_{yz} \leq 5$) are the most common expression of the folds. The tubes are elongate subparallel to stretching lineation and are defined by centimeter-scale layers of schist. Eccentrically nested elliptical patterns and opposing asymmetry of folds ('S' and 'Z') are consistent with the sheath-fold interpretation. Sheath folds are locally numerous in the Moretti-Harrah quarry but are not widely distributed in the Sylacauga Marble Group; reconnaissance in neighboring quarries provided no additional observations.

The presence of sheath folds in part of the Talladega slate belt indicates a local history of plastic, non-coaxial deformation. Such a history of deformation is substantiated by petrographic study of an extracted hinge from the Moretti-Harrah quarry. The sheath folds are modeled as due to passive amplification of initial structures during simple shear, using both analytic geometry and graphic simulation. As indicated by these models, relatively large shear strains ($\gamma \geq 9$) and longitudinal initial structures are required. The shear strain presumably relates to NW-directed displacement of overlying crystalline rocks during late Paleozoic orogeny.

INTRODUCTION

SHEATH folds have been widely recognized in recent years, particulary in well-exposed ductile shear zones where rocks have deformed plastically and where the strain path is thought to have approximated simple shear (e.g. Carreras *et al.* 1977, Rhodes & Gayer 1977, Williams 1978, Minnigh 1979, Henderson 1981, Evans & White 1984, Lacassin & Mattauer 1985, Skjernaa 1989, Fossen & Rykkelid 1990). In the deeply eroded southern Appalachians, such geologic environs include the Brevard, Goat Rock, Modoc, Nutbush Creek and Towaliga fault zones, to name but a few. Despite the commonness of ductile shear zones in this region, very few sheath folds have been documented (e.g. Steltenpohl 1989, p. 26, fig. 1-18 in Mies 1990).

The intent of this paper is to describe observations made in the Moretti-Harrah quarry, as they relate to the present interpretation of sheath folds, and to explore the significance of sheath folds in the Sylacauga Marble Group. The sheath folds are modeled as due to simple shear deformation of pre-existing or shear-related folds using analytic geometry and graphic simulation. The models are used to estimate shear strain and to identify the range of potential initial structures.

FOLDS IN THE MORETTI-HARRAH QUARRY

About the quarry

The Moretti-Harrah marble quarry (3,669,050 m north, 566,700 m east, UTM grid zone 16) is located near Sylacauga, Talladega County, Alabama. The quarry was initially opened in 1912 for the production of building and monument stone (Prouty 1916) and is presently operated by E.C.C. America Incorporated. In recent years, dimension-stone operations were replaced by the production of crushed and ground (micronized) marble that is blasted, rather than cut, from the quarry walls. Remnant quarry blocks, utilized extensively in the present study, occur in dumps and along the quarry roads.

The quarry stone is white calcite marble with discontinuous layers of muscovite schist, typically 1 to a few centimeters thick and irregularly spaced at intervals of 1 to several meters. The schist layers define a foliation that dips 20–35° toward the southeast (150–160°) and contains a mineral aggregate (stretching) lineation that plunges 25–30°, also toward the southeast (130–150°). These orientations are typical of foliation and lineation in the region.

Geologic setting

The Moretti-Harrah quarry occurs in the Lower Cambrian to Lower Ordovician Sylacauga Marble Group, a greenschist-facies metacarbonate sequence in the Talladega slate belt (Tull 1982) (Fig. 1). More specifically, the quarry occurs in the lower white marble member (Guthrie 1989) of the Gantts Quarry Formation (Tull 1985) (Fig. 2).

The Sylacauga Marble Group is stratigraphically underlain by the Upper Precambrian to Lower Cambrian Kahatchee Mountain Group and is overlain, in succession, by the Silurian to Lower Devonian Talladega Group and the Hillabee Greenstone (Fig. 2). Collectively, these rocks comprise the Talladega slate belt, which is bounded to the northwest, against the foreland fold and thrust belt, by the Talladega–Cartersville fault system (Hayes 1891, McCalley 1897, Tull 1982). To the southeast, the Talladega slate belt is bounded by the Hollins line fault and is overlain by the

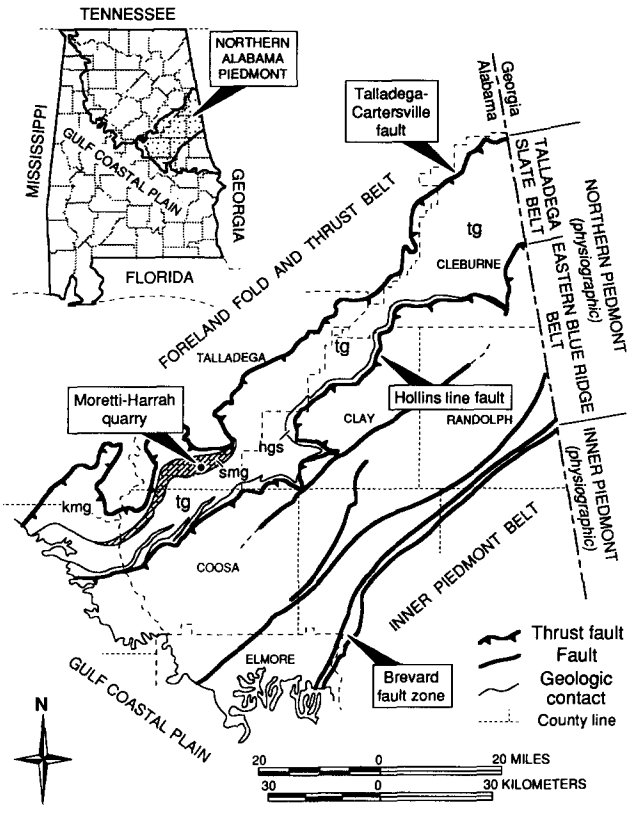

Fig. 1. Simplified geologic map of the northern Alabama Piedmont (modified after Tull 1978, Osborne *et al.* 1988). hgs = Hillabee Greenstone; kmg = Kahatchee Mountain Group; smg = Sylacauga Marble Group (also carbonate pattern); tg = Talladega Group. Note the location of the Moretti-Harrah quarry.

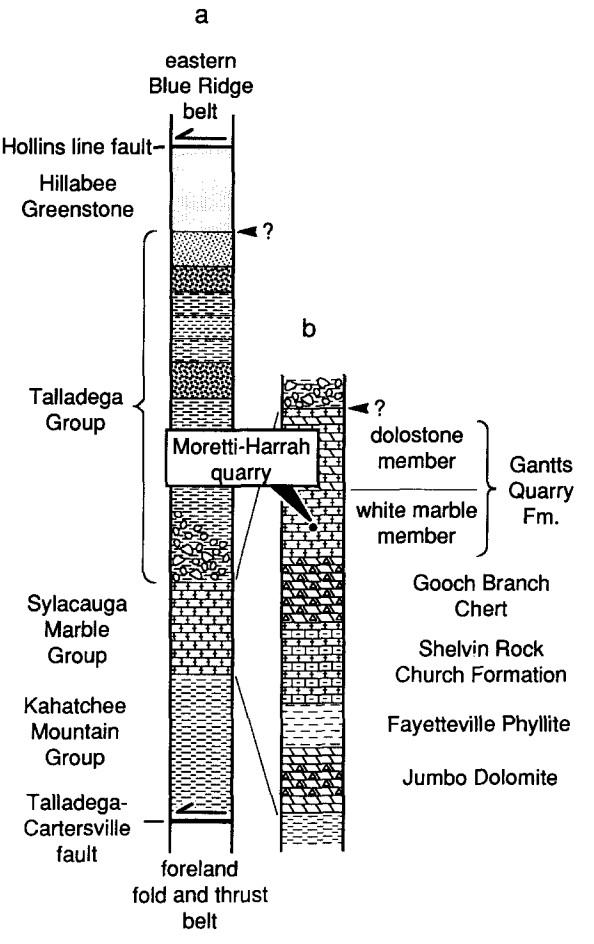

Fig. 2. (a) Stratigraphic–structural framework of the Talladega slate belt (modified after Tull 1982) and (b) detailed stratigraphy of the Sylacauga Marble Group (modified after Tull 1985, Guthrie, 1989). Debated stratigraphic or tectonic boundaries are queried. Note the structural and stratigraphic location of the Moretti-Harrah quarry.

eastern Blue Ridge belt (Hatcher 1978, Tull 1978, 1982, Steltenpohl & Moore 1988) (Fig. 1).

The Kahatchee Mountain and Sylacauga Marble Groups record a rift to drift succession of tectonic processes during the late Precambrian and early Paleozoic (Tull & Guthrie 1985). The Sylacauga Marble Group is biostratigraphically correlated with the unmetamorphosed Cambrian to Ordovician carbonate platform of the foreland (Harris *et al.* 1984, Tull & Guthrie 1985) and is interpreted as a distal fragment of the Laurentian miogeocline that was thrust onto more proximal facies during late Paleozoic orogeny (Tull *et al.* 1988).

Methods of observation and analysis

Structures in the marble, both in the quarry wall (*in situ*) and in remnant quarry blocks, were observed and photographed during June 1991. Orthogonal sections provided by meter-scale rectangular blocks were particularly useful to three-dimensional interpretation. Twelve blocks were studied in detail with the aid of high-contrast, black and white photographs. Typically, seven frames were taken of each block; one taken orthogonal to each of the five available surfaces (top, two sides, and two ends, Fig. 3) and two taken from approximate isometric perspectives.

Photographs of quarry blocks allowed for complete geometric analysis of structures in the laboratory. Also, photographs taken of the quarry wall from up- or down-structure perspectives (25–30° from horizontal) were used to eliminate distortion in oblique sections and to side-step difficulties of measurement along irregular surfaces.

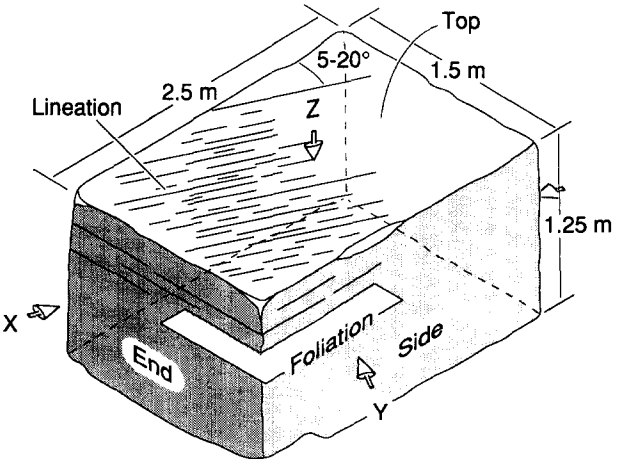

Fig. 3. Schematic illustration showing the approximate orientations of finite strain axes (X, Y and Z) in remnant quarry blocks as interpreted from foliation and stretching lineation. X and Y form small angles (5–20°) with the length and width of the block. The XY plane is parallel to the top of the block. Approximate dimensions of the block are also shown.

Sheath folds

Intrafolial, meter-scale, marble "lenses", "separated from the marble mass by a film of muscovite schist", were described from marble blocks at the Moretti-Harrah quarry by Dale (1921) and were illustrated by Prouty (1916, plates 25 and 26). Based on the preponderance of elliptical sections on orthogonal surfaces, Dale interpreted an ellipsoidal three-dimensional form. Both authors attributed these structures to intrafolial 'drag folding', which Dale conceded does not fully explain isolated ellipsoids.

The elliptical patterns are presently interpreted as due to slightly oblique longitudinal sections and cross-sections of marble tubes. The tubes are elongate approximately parallel to stretching lineation. In most blocks, the intervening angle is indiscernible or poorly constrained. Long axes of elliptical cross-sections ($4 \leq R_{yz} \leq 5$) are parallel to foliation (Fig. 4).

Most of the meter-scale rectangular blocks that partially contain these tubes were cut from the quarry with two surfaces (top and bottom) parallel to foliation (approximate XY plane of finite strain) and with their long dimensions at a small angle (5–20°) to stretching

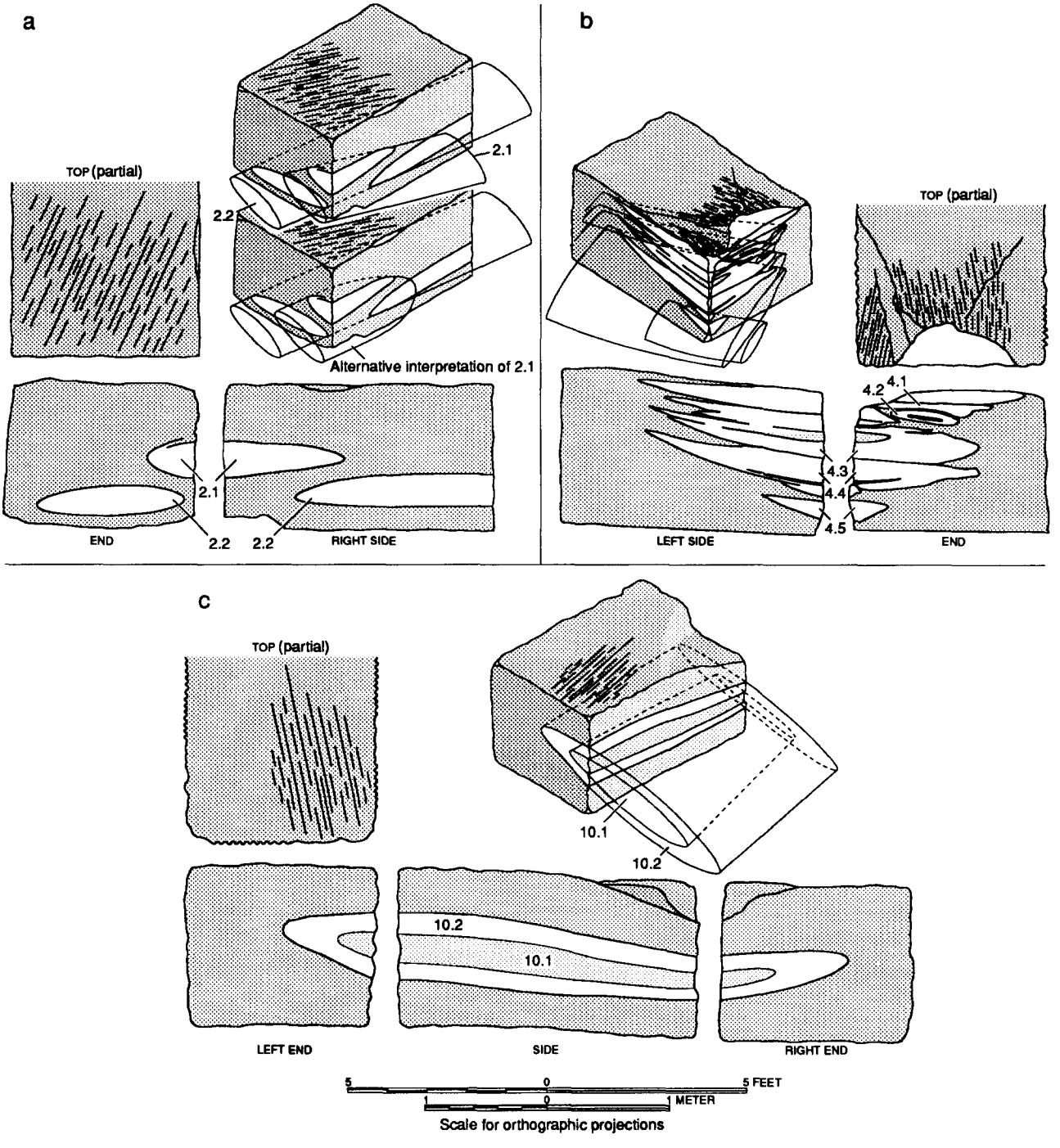

Fig. 4. Orthographic and isometric projections of remnant quarry blocks 2, 4, and 10 (a, b and c). Isometric projections (scaled 60%) show interpretations of marble tubes. Shading is used to emphasize the elliptical patterns. Note the nested tubes in (c) (10.1, inner tube; 10.2, outer tube) and eccentrically nested tubes within 4.2 and 4.3 in (b). The lower isometric projection in (a) shows an alternative interpretation of tube 2.1 as the cap of a sheath fold.

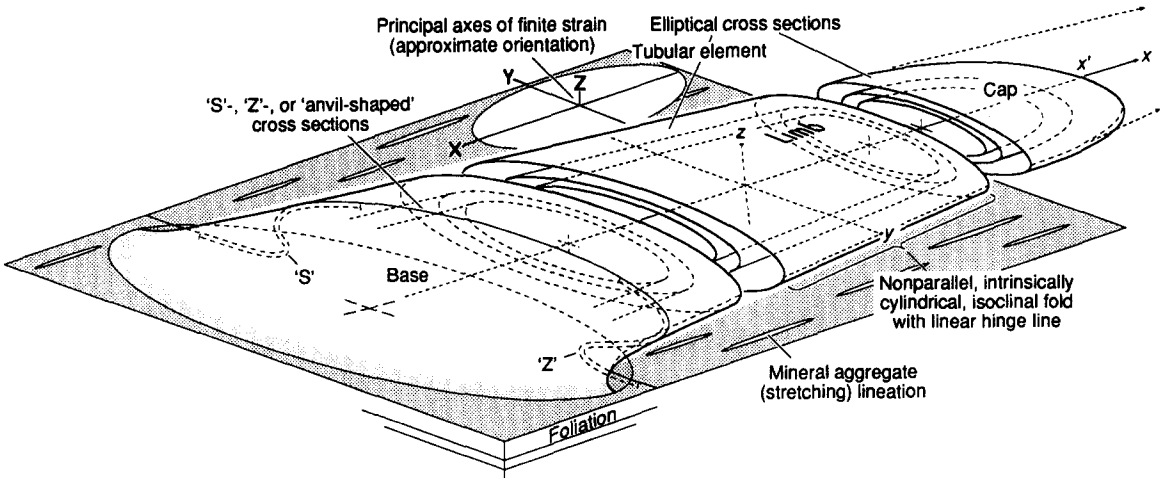

Fig. 5. Schematic illustration of an idealized sheath fold fashioned after observations made at the Moretti-Harrah quarry. The structure is oriented as though in a horizontal shear zone. The reference frame (x, x', y, z, lower-case italic typeface) was adapted from Minnigh (1979); note the relation to principal axes of finite strain (X, Y and Z, upper-case).

lineation (approximate X direction), such that all surfaces perpendicular to foliation (sides and ends, Fig. 3) provide elliptical sections. The reason for this relationship is uncertain. The low-angle intersection of lineation in quarry blocks may have been intentional, in order to accentuate patterns caused by schist in the marble, or it may have been dictated by some other control, such as joints (Prouty 1916, p. 76). Alternatively, this may have been an undesirable configuration due to local variation of rock fabric and may have contributed to the rejection of blocks that remain at the quarry.

The tubes are here interpreted as parts of sheath folds (Fig. 5). Although the full length of a sheath (x') has not been observed, one analysis indicated $x':y:z = >6:1:0.26$. This is a *tubular fold* by Skjernaa's (1989) definition. However, the author finds the term *sheath fold* more descriptive in the present case.

The sheath-fold interpretation was inspired, in part, by the observation of eccentrically nested elliptical patterns (Fossen & Rykkelid 1990). In a few cases, the marble tubes are composite, such that similarly proportioned and similarly oriented elliptical patterns occur in cross-section, one nested inside the other ('eye folds', e.g. Dalziel & Bailey 1968, Lacassin & Mattauer 1985) (Fig. 6). In every such case, the ellipses are eccentric (i.e. without a common center) and share a plane of approximate bilateral symmetry that contains their minor axes. By various models (e.g. Skjernaa 1989, fig. 14 in Fossen & Rykkelid 1990, present paper), this observation can be attributed to a relative thinning or thickening of one limb.

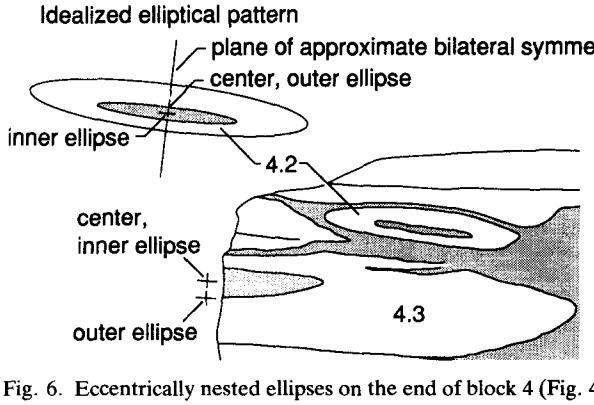

Fig. 6. Eccentrically nested ellipses on the end of block 4 (Fig. 4b).

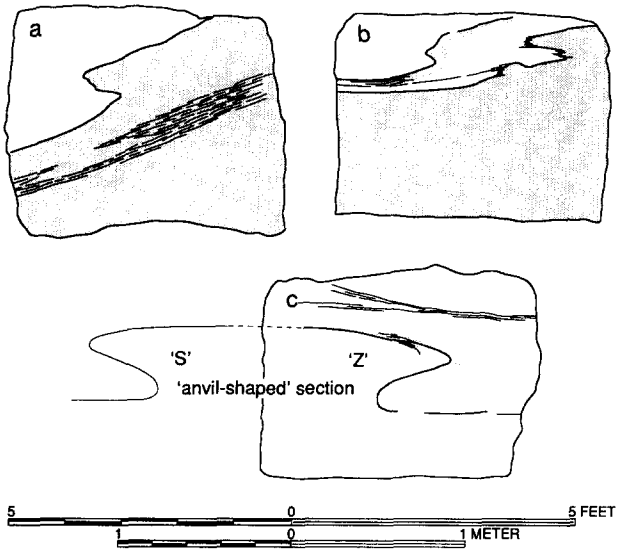

Fig. 7. Sketches of 'S' and 'Z' patterns observed on the ends of blocks 1, 7 and 3 (a, b and c). These structures are viewed nearly parallel to stretching lineation (X direction) on the top surfaces of each block. The hypothetical 'S' pattern shown adjacent to block 3 in (c) complements the 'Z' pattern observed on the end of the block. The combination of 'S' and 'Z' patterns forms an 'anvil-shaped' cross-section (Fig. 5).

Opposed asymmetry of folds was observed in the quarry wall and 'S' and 'Z' patterns were found on the ends of several blocks (Fig. 7), although *in situ* orientations of the blocks are unknown. These features are interpreted as parts of the characteristic 'anvil-shaped' section, found at the base of a sheath fold (Figs. 5 and 7).

Conceptually, the tubular element of the sheath comprises two, intrinsically cylindrical, isoclinal folds jointed at the limbs (Fig. 5). One of these folds was extracted from rubble at the Moretti-Harrah quarry (Fig. 8). A thin layer of schist defines the fold, which has a remarkably linear hinge line (axis) that lies subparallel to stretching lineation. White mica in the schist is fully

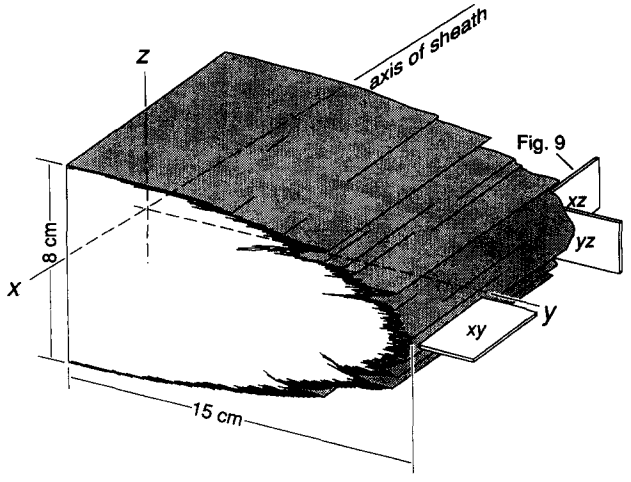

Fig. 8. Sketch of an extracted isoclinal fold, as occurs at vertices of marble tubes. The fold is defined by a layer of schist (shaded) and the core of the fold contains white marble. Mica in the schist is fully polygonized such that {001} (schistosity) approximates the axial (*xy*) plane. The reference frame (*x*, *y*, *z*) is related to a sheath fold in Fig. 5.

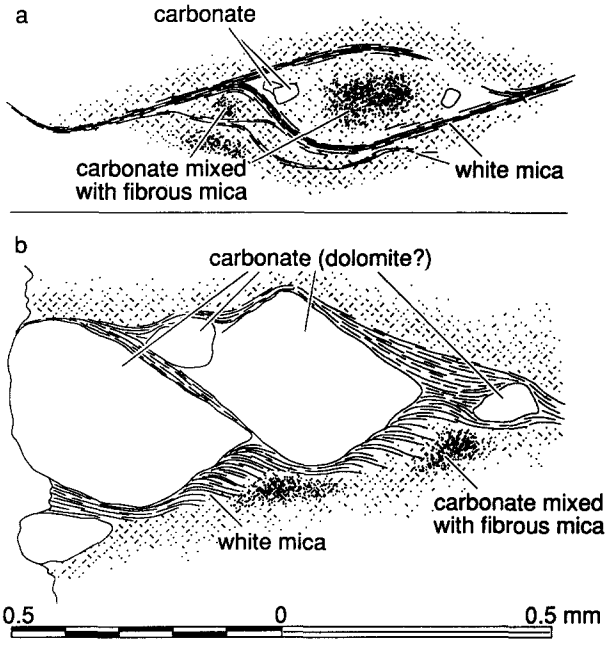

Fig. 9. Examples of submillimeter-scale structures observed in thin sections cut in the *xz* plane from the hinge of an extracted fold (Fig. 8). (a) Sigmoidal structure that resembles a σ-type porphyroclast (Passchier & Simpson 1986) or the pattern of schistosity between shear bands (Simpson 1986). (b) Broken and antithetically displaced carbonate grain (Simpson & Schmid 1983, Simpson 1986); the segments have a constant crystallographic orientation.

polygonized such that {001} approximates the axial (*xy*) plane. Hence, the mica is interpreted as part of the neoblastic assemblage related to sheath fold development.

Petrographic study of the extracted fold revealed submillimeter-scale structures that are traditionally related to non-coaxial deformation (e.g. Simpson & Schmid 1983, Lister & Snoke 1984, Simpson 1986) (Fig. 9). These structures are particularly evident in thin sections cut in the *xz* plane from the schistose hinge of the fold (Fig. 8). This corroborates a non-coaxial strain path, as is commonly thought to have attended sheath fold development (e.g. Carreras *et al.* 1977, Rhodes and Gayer 1977, Lacassin & Mattauer 1985, Skjernaa 1989). These observations are also consistent with the inferred geometric relation of the fold and axes of finite strain; the *xz* plane of the fold (Figs. 5 and 8) apparently contains the *XZ* principal section (Figs. 3 and 5). Other than small-scale structures illustrated by Fig. 9, there is very little textural or microstructural evidence of deformation in the marble; calcite grains are equant to slightly elongate in the *x* direction, 0.15–0.40 mm in diameter, have smooth grain boundaries with a preponderance of 120° grain-boundary triple junctions, exhibit uniform (nonundulose) extinction, and only 20% of the grains are twinned. Apparent annealing of the calcite can be interpreted to indicate intracrystalline deformation during metamorphic conditions (Schmid *et al.* 1987, p. 774), in this case of the greenschist facies (Tull *et al.* 1988, Guthrie 1989).

Axial culminations or *caps* of sheath folds (Fig. 5) have not been positively identified in the present case. The absence of this observation is not unusual (e.g. Rhodes & Gayer 1977, La Tour 1981, Evans & White 1984) and can be attributed to the fact that the cap forms only a small part of the sheath. Recognition of the cap is difficult in the absence of three-dimensional forms.

PASSIVE-AMPLIFICATION MODELS

It is well established that sheath folds, including the tubular folds of Skjernaa (1989), commonly occur in ductile shear zones and that simple shear may dominate progressive deformation leading to such structures (e.g. Carreras *et al.* 1977, Rhodes & Gayer 1977, Cobbold & Quinquis 1980, Ghosh & Sengupta 1984, 1987, Vollmer 1988, Skjernaa 1989, Fossen & Rykkelid 1990). Non-coaxial deformation is indicated in the present case by submillimeter-scale structures observed in thin section (Fig. 9) and by the relation of macroscopic foliation and stretching lineation (approximate *X* direction) (Figs. 3 and 5). Hence, it is believed that simple shear was operative during the evolution of sheath folds at the Moretti-Harrah quarry.

As in models cited above, passive behavior (i.e. homogeneous flow) is assumed. Considering the wide spacing of thin schistose layers in the marble and the well-known plastic behavior of carbonates and mica at greenschist-facies metamorphic conditions (e.g. Rutter 1974, Ramsay 1982), the layering may not have been rheologically significant.

Geometric model

The present model (Fig. 10), evaluated using analytic geometry, a microcomputer and the APL language, is fashioned after Skjernaa (1989) and utilizes many of the same conventions and symbols. The model considers the specific case of horizontal simple shear acting on a symmetric perturbation in an otherwise horizontal sur-

face, hereafter referred to as the *initial structure*. Three types of initial structures are considered. Initial structures with an elliptical horizontal section are non-cylindrical, periclinal folds. In *longitudinal* folds, the major axis of the horizontal section is parallel to the shear direction. In *transverse* folds, the major axis is perpendicular to the shear direction; the terminology used here does not, then, conform with that proposed by

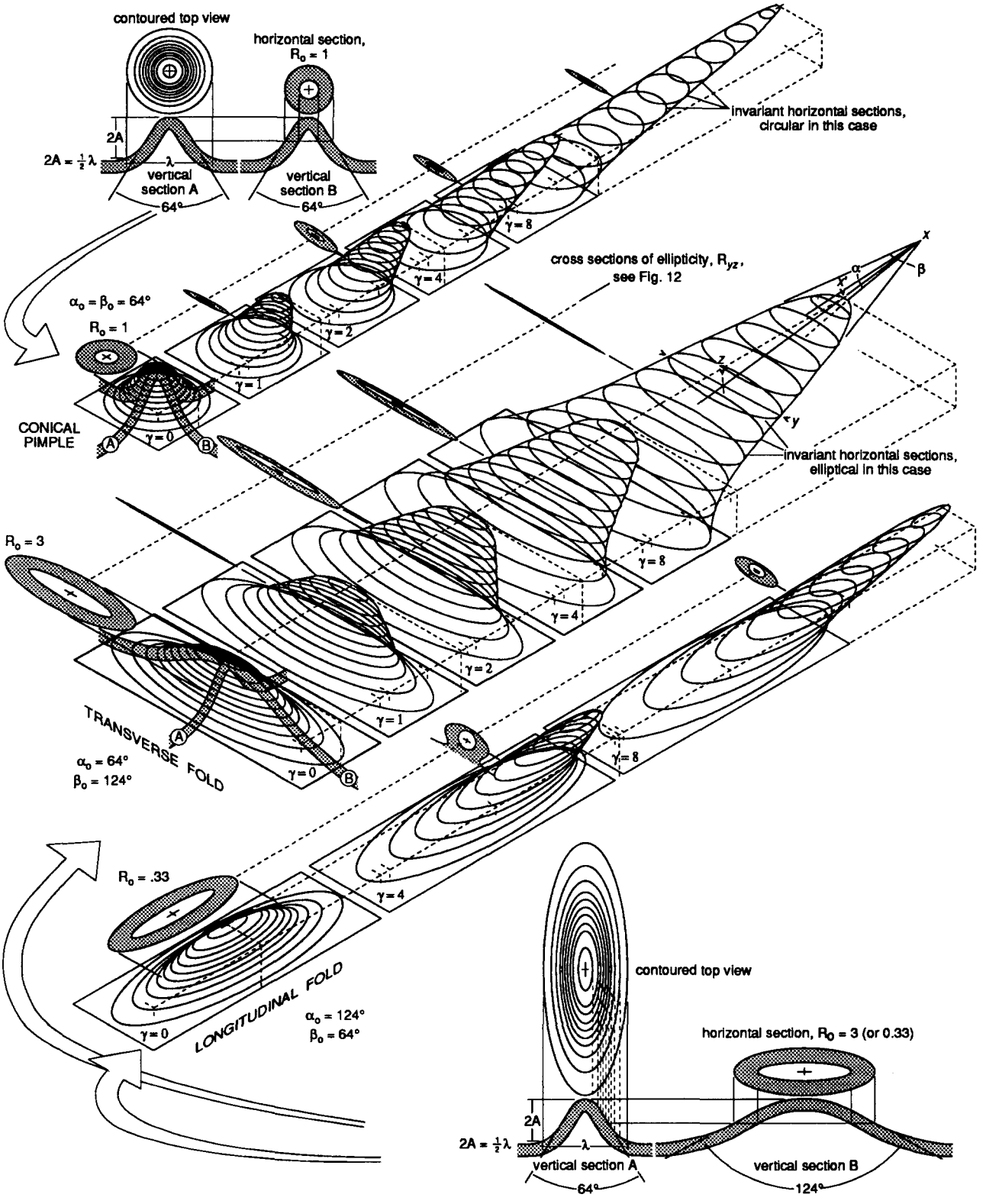

Fig. 10. Passive-amplification sheath fold models. Initial structures with $2A = \frac{1}{2}\lambda$ (A = amplitude, λ = wavelength) are shown in orthographic projections (three views plus horizontal section). Isometric projections show progressive deformation of initial structures due to horizontal simple shear ($\gamma = 0$–8). Graphic simulations using $R_o = 1, 1.5, 2$ and 3 (0.66, 0.5 and 0.33, in the case of longitudinal folds) were performed with results that closely match the conceptual model of Skjernaa (1989) (see Fig. 11); *yz* cross-sections are shown in Fig. 12. The reference frame (x, x', y, z, lower-case italic typeface) is shown for $R_o = 3$ (also see Fig. 5). Apical angles of resulting structures, α and β, are measured in *xz* and *xy* planes; α_o and β_o are measured in the incipient *xz* and *xy* planes.

Skjernaa (1989). The third type of initial structure is a *conical pimple* with a circular horizontal section.

Resultant sheath folds are described using a modification of Minnigh's (1979) reference frame (Figs. 5 and 10), where x (lower case) is the central axis of the sheath and extends beyond the cap to the apex of a cone that is tangent to the sheath at inflection points. x' is the segment of x contained within the sheath, i.e. the length of the sheath measured from the center of the base, such that $\frac{1}{2}x'$ = amplitude. y and z are dimensions of the elliptical section cut normal to x at the midpoint in the length of the sheath (x') and are measured parallel to major and minor axes (see also the Appendix). Additionally, x, y and z are orthogonal and, for starting configurations presently considered, y is parallel to the Y direction of finite strain. x and z approximate the X and Z directions at high strains. The angles α and β lie between the limbs and between the hinges of the sheath and are measured in the xz and xy planes, respectively (Skjernaa 1989) (Fig. 10); in both cases, x is the bisector. α_o and β_o are corresponding angles in the initial structure.

During passive amplification of initial structures, R_{yz} changes as a function of γ and initial values of α and β. This is described by the equation

$$\beta_o = 2\tan^{-1}\left[\tan\left(\frac{\left[\tan^{-1}\left(\gamma - \tan\frac{\alpha_o}{2}\right)^{-1}\right] - \left[\tan^{-1}\left(\tan\frac{\alpha_o}{2} + \gamma\right)^{-1}\right]}{2}\right) \cdot R_{yz}\left(\cos\tan^{-1}\gamma\right)^{-1}\right], \quad (1)$$

which is a combination of Skjernaa's (1989) equations (A3) and (A6) (see Appendix). Solutions to equation (1), using $R_{yz} = 4$, $R_{yz} = 5$ and $\gamma = 1, 2, 3, \ldots, 6, 8, 10, 14, 20, 30$ and 50 are plotted in Fig. 11.

Graphs in Fig. 11 show combinations of α_o, β_o and γ (contoured) that result in specific values of R_{yz}. A line that has a slope of 1 and passes through the origin represents a conical pimple ($R_o = 1$, $\alpha_o = \beta_o$) and separates fields of transverse ($\beta_o > \alpha_o$) and longitudinal ($\alpha_o > \beta_o$) initial structures. Graphs for $R_{yz} = 4$ (Fig. 11a) and $R_{yz} = 5$ (Fig. 11b) represent the range of R_{yz} presently observed and provide limiting combinations of α_o, β_o and γ, i.e. ranges of initial structures and the shear strain required to produce $4 \leq R_{yz} \leq 5$. For example, conical pimples with apical angles less than 90° require $4 \leq \gamma \leq 5$. In general, transverse initial structures require less shear strain and longitudinal initial structures require greater shear strain.

An added constraint is the length of the sheath, x'. In the present case, $x' \geq 6y$ was observed. Although the fraction x'/x varies as a function of curvature at the cap, a value of 0.8 was assumed. This being the case, the condition $x' \geq 6y$ requires $\beta \leq 7.6°$. Skjernaa's (1989) equation A6 (see Appendix) can be rearranged to give

$$\beta_o = 2\tan^{-1}\left[\left(\tan\frac{\beta}{2}\right)\left(\cos\tan^{-1}\gamma\right)^{-1}\right], \quad (2)$$

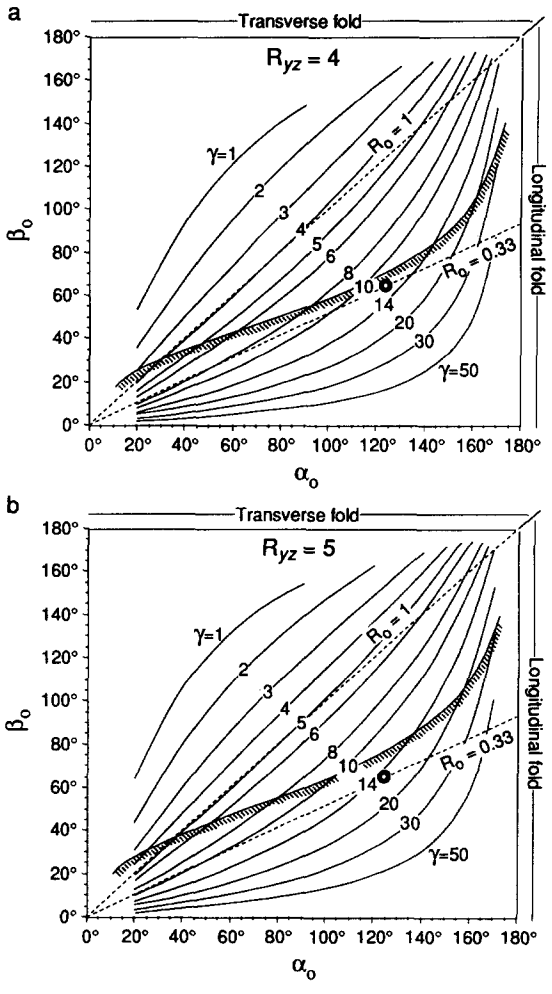

Fig. 11. Plot of α_o against β_o for structures that, when subjected to horizontal simple shear (γ contoured), result in (a) $R_{yz} = 4$ and (b) $R_{yz} = 5$. Hachured curves mark $\beta = 7.6°$. As required by the present model, initial structures at the Moretti-Harrah quarry plot below these curves ($\beta \leq 7.6°$, $x' \geq 6y$). The longitudinal fold ($R_o = 0.33$) shown in Fig. 10 is plotted as bold, open circles. Computations were made using a combination of equations derived by Skjernaa (1989) (see Appendix) and have been tested against graphic simulations (Fig. 12, for example).

solutions for which, with $\beta = 7.6°$, have been plotted in Fig. 11 (hachured curves). Using the present model, initial structures that plot below the hachured curves will yield sheath folds like those observed at the Moretti-Harrah quarry, if subjected to the indicated (contoured) shear strain.

It is readily apparent from Fig. 11 that sheath folds at the Moretti-Harrah quarry evolved from initially longitudinal, non-cylindrical folds and that $\gamma \geq 9$ is required, assuming that initial structures were relatively open. A longitudinal fold having $R_o = 0.33$, $\alpha_o = 124°$ and $\beta_o = 64°$, as shown in Fig. 10 and plotted in Fig. 11, for example, is a possible initial structure and requires $12 \leq \gamma \leq 15$.

Graphic simulation

Graphic simulations, performed using the homogeneous simple shear (skew) capability of common graphics/CAD microcomputer programs, provide a test of the

analytic geometry and visualization of the passive-amplification process (Fig. 10). Results of the simulations, particularly in terms of R_{yz} (Fig. 12), closely match predictions of the geometric model (Fig. 11) and corroborate conclusions based thereon.

Additionally, Fig. 12 illustrates one way to develop the eccentrically nested elliptical sections observed at the Moretti-Harrah quarry (see also figs. 2c, 3c and A1b in Skjernaa 1989). By the present model, this is due to differential compression and extension of the limbs, resulting in a relatively short, thick limb and a relatively long, thin limb. Although both limbs ultimately lie in the extension field of incremental strain, only the 'inverted' limb is first shortened and remains the thicker of the two limbs. The difference in limb thickness becomes progressively less after the inverted limb enters the extension field. This relation will be found in sheaths produced by passive amplification during simple shear of a symmetric perturbation in a surface that is otherwise parallel or close to the shear plane.

A monoclinal flexure in the same surface, inclined in the direction of homogeneous flow, will undergo a

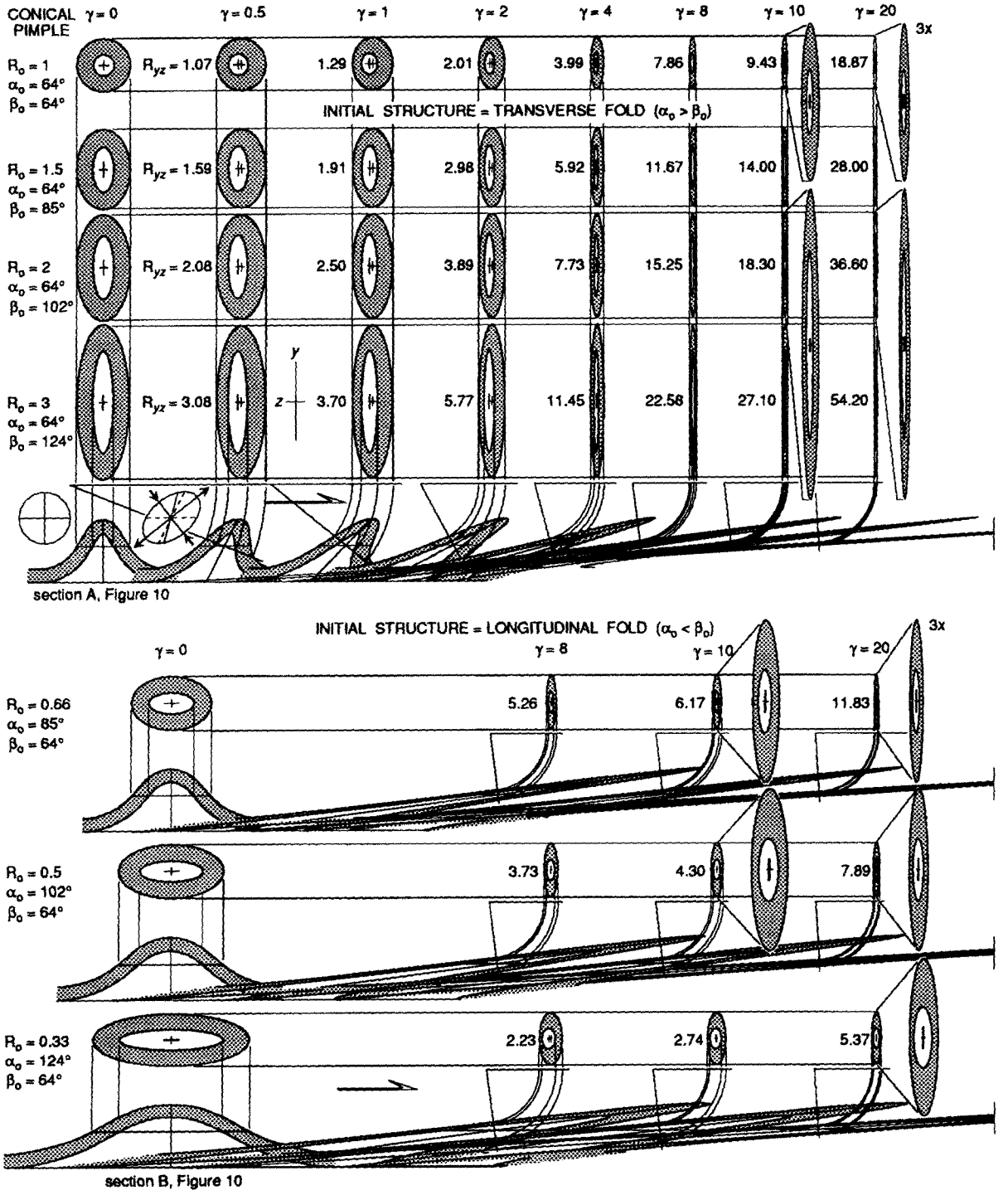

Fig. 12. Elliptical patterns (R_{yz}) resulting from graphic simulations illustrated above and by Fig. 10. Note the eccentricity of nested ellipses due to differential attenuation and compression of the limbs.

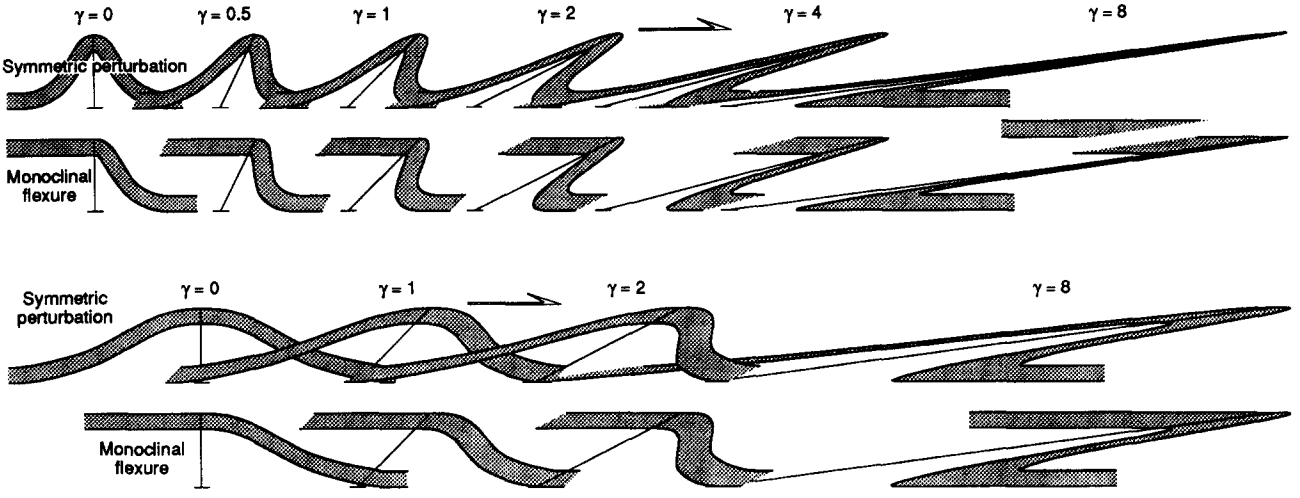

Fig. 13. Passive amplification of symmetric perturbations (Figs. 10 and 12) and monoclinal flexures. Sections are parallel to the movement direction. Note differences of limb-thickness relations at advanced stages of deformation.

sequence of deformation similar to that of the inverted limb in the present model (Fig. 13). However, in this case, the 'upright' limb remains parallel to the plane of no finite longitudinal strain, while the inverted limb is extended at advanced stages of deformation. Consequently, the inverted limb becomes the thinner of the two limbs and the difference in limb thickness increases (cf. fig. 14 in Fossen & Rykkelid 1990). As pointed out by Fossen & Rykkelid (1990), eccentrically nested elliptical sections are potential sense-of-shear indicators if the direction to the cap or base of the fold is known. However, the geometry of the initial perturbation can radically affect limb-thickness relations and the eccentricity of nested elliptical sections. Unfortunately, this aspect of the present model could not be tested because none of the composite sheath folds observed at the Moretti-Harrah quarry were accompanied by sense-of-shear indicators and only a few poorly exposed examples were observed *in situ*.

DISCUSSION

The present application of Skjernaa's (1989) geometric model corroborates one of her principal conclusions—that initially longitudinal folds (transverse folds in her terminology) are required for the evolution of tubular folds by passive amplification due to simple shear. Applied to sheath folds in general, this concept is inconsistent with a conventional model for their development, whereby the initial structure has a contemporary origin (i.e. shear related, Escher & Watterson 1974, see also Carreras *et al.* 1977) and a transverse orientation (e.g. Rhodes & Gayer 1977, Ghosh & Sengupta 1984, 1987). It is interesting to note in this context that relatively open folds of mylonitic foliation with axes approximately parallel to stretching lineation have been described and have been interpreted as having initiated in the longitudinal orientation (e.g. Bell & Hammond 1984, Ghosh & Sengupta 1987).

Potential combinations of initial structures and shear strains required for sheath folds like those presently observed were determined using α_o–β_o–γ plots based on the geometric model (Fig. 11). Such diagrams, customized for observed sheath-fold cross-sectional ellipticity (R_{yz}), make it possible to speculate as to initial structures and required shear strains, and provide a case-specific alternative to fig. 4 in Skjernaa (1989). The model can be further customized, giving more refined results, using additional constraints such as length of the sheath (x', relative to y), as in the present case, or interlimb (α) and interhinge (β) angles, etc., as available.

Although simple shear is not required for the evolution of sheath folds (e.g. Borradaile 1972, Ramsay 1979), it is indicated in many cases (e.g. Carreras *et al.* 1977, Rhodes & Gayer 1977, Gobbold & Quinquis 1980, Ghosh & Sengupta 1984, 1987, Vollmer 1988, Skjernaa 1989, Fossen & Rykkelid 1990). Considering corroborative petrographic evidence and macroscopic fabrics presently described, sheath folds at the Moretti-Harrah quarry are interpreted to have evolved during dominantly simple shear deformation. The magnitude of such deformation following the initial perturbation, $\gamma \geq 9$, is constrained by the present model. However, the extent of this deformation is largely unknown due to relatively poor exposure and irregular distribution of the sheath folds. Recognition of a non-coaxial strain path may also be hindered by the tendency of calcite to become annealed at greenschist facies or higher metamorphic conditions, obliterating characteristic textures and microstructures in the marble (Schmid *et al.* 1987, p. 774).

By using the sheath folds presently described as a means of recognizing and quantifying a history of simple shear in the marble at Sylacauga, it is concluded that such deformation is localized in part of the Moretti-Harrah quarry, as in a SE-dipping ductile shear zone. Delineated by the presence of sheath folds, this shear zone is approximately 30 m thick, which corresponds to

a displacement of *at least* 270 m using $\gamma \geq 9$. This deformation is interpreted as related to the Talladega–Cartersville fault system (Tull 1982, p. 6), which, as presently construed, includes major thrusts in and adjacent to the Sylacauga Marble and Kahatchee Mountain Groups as well ductile deformation zones and possible antithetic ('late') faults recognized by Guthrie (1989). Although there has been considerable debate as to the location(s) of this fault system and names of its constituents (e.g. Shaw 1970, Carrington 1973, Thomas & Neathery 1980, Tull 1982, Guthrie 1989, 1990), most authors agree that faults at this structural position relate to NW-directed displacement of overlying crystalline rocks during late Paleozoic orogeny.

CONCLUSIONS

Meter-scale elliptical patterns and related observations in the Moretti-Harrah dimension-stone quarry are two-dimensional expressions of sheath folds. The presence of sheath folds in part of the Sylacauga Marble Group, plus corroborating evidence, indicates a local history of plastic, non-coaxial deformation interpreted as due to NW-directed displacement of overlying crystalline rocks during late Paleozoic orogeny. When modeled as due to passive amplification of initial structures during simple shear, using both analytic geometry (Skjernaa 1989) and graphic simulation, sheath folds at the Moretti-Harrah quarry require longitudinal initial structures and $\gamma \geq 9$.

Acknowledgements—The author wishes to thank David Leverett of E.C.C. America Incorporated and Jimmy Reynolds of Georgia Marble Company for access to the respective marble quarries and for their assistance in locating material suitable to the present study. Christopher Talbot, Frederick Vollmer and Steven Wojtal provided helpful criticism of the manuscript. Thanks are also due to Kevin Stewart and Greg Guthrie for their comments on the original draft. Support for this research was provided by the Geological Survey of Alabama.

REFERENCES

Bell, T. H. & Hammond, R. L. 1984. On the internal geometry of mylonite zones. *J. Geol.* **92**, 667–686.

Borradaile, G. J. 1972. Variably oriented co-planar primary folds. *Geol. Mag.* **109**, 89–98.

Carreras, J., Estrada, A. & White, S. 1977. The effects of folding on the C-axis fabrics of a quartz mylonite. *Tectonophysics* **39**, 3–24.

Carrington, T. J. 1973. Metamorphosed Paleozoic sedimentary rocks in Chilton, Shelby, and Talladega Counties, Alabama. In: *Talladega Metamorphic Front* (edited by Carrington, T. J.) *Alabama Geol. Soc. 11th Ann. Field Trip Guidebook*, 22–38.

Cobbold, P. R. & Quinquis, H. 1980. Development of sheath folds in shear regimes. *J. Struct. Geol.* **2**, 119–126.

Dale, T. N. 1921. On concentric drag-folding in Alabama marble. *Am. J. Sci.* **2**, 319–321.

Dalziel, I. W. D. & Bailey, S. W. 1968. Deformed garnets in a mylonitic rock from the Grenville front and their tectonic significance. *Am. J. Sci.* **266**, 542–562.

Escher, A. & Watterson, J. 1974. Stretching fabrics, folds and crustal shortening. *Tectonophysics* **22**, 223–231.

Evans, D. J. & White, S. H. 1984. Microstructural and fabric studies from the rocks of the Moine Nappe, Eriboll, NW Scotland. *J. Struct. Geol.* **6**, 369–389.

Fossen, H. & Rykkelid, E. 1990. Shear zone structures in the Øygarden area, west Norway. *Tectonophysics* **174**, 385–397.

Ghosh, S. K. & Sengupta, S. 1984. Successive development of plane noncylindrical folds in progressive deformation. *J. Struct. Geol.* **6**, 703–709.

Ghosh, S. K. & Sengupta, S. 1987. Progressive development of structures in a ductile shear zone. *J. Struct. Geol.* **9**, 277–287.

Guthrie, G. M. 1989. Geology and marble resources of the Sylacauga Marble District. *Bull. Alabama geol. Surv.* **131**.

Guthrie, G. M. 1990. Geologic setting of the foreland–hinterland transition zone in the southern and central Appalachians. In: *Contrasts in Structural Styles and Mechanisms in a Foreland–Hinterland Transition Zone, Central Alabama Appalachians* (edited by Guthrie, G. M. & Osborne, W. E.). *Geol. Soc. Am. 39th Ann. M., Southeastern Sect. Field Trip II Guidebook*. Alabama Geological Survey, 1–16.

Harris, A. G., Repetski, J. E., Tull, J. F. & Bearce, D. N. 1984. Early Paleozoic conodonts from the Talladega slate belt of the Alabama Appalachians: tectonic implications. *Geol. Soc. Am. Abs. w. Prog.* **16**, 143.

Hatcher, R. D., Jr. 1978. Tectonics of the western Piedmont and Blue Ridge, southern Appalachians: review and speculation. *Am. J. Sci.* **278**, 276–304.

Hayes, C. U. 1891. The overthrust faults of the southern Appalachians. *Bull. geol. Soc. Am.* **2**, 141–154.

Henderson, J. R. 1981. Structural analysis of sheath folds with horizontal X-axes, northeast Canada. *J. Struct. Geol.* **3**, 203–210.

Lacassin, R. & Mattauer, M. 1985. Kilometre-scale sheath folds at Mattmark and implications for transport directions in the Alps. *Nature* **315**, 739–741.

La Tour, T. E. 1981. Significance of folds and mylonites at the Grenville Front in Ontario. *Bull. geol. Soc. Am.* **92**, 411–413.

Lister, G. S. & Snoke, A. W. 1984. S–C mylonites. *J. Struct. Geol.* **6**, 617–638.

McCalley, H. 1897. Report on the valley regions of Alabama, Part II, the Coosa Valley region. *Spec. Rep. Alabama geol. Surv.* **9**.

Mies, J. W. 1990. Structural and petrologic studies of mylonite at the Grenville basement–Ashe Formation boundary, Grayson County, Virginia to Mitchell County, North Carolina. Unpublished Ph.D. thesis, University of North Carolina, Chapel Hill.

Minnigh, L. D. 1979. Structural analysis of sheath folds in a meta-chert from the western Italian Alps. *J. Struct. Geol.* **1**, 275–282.

Osborne, W. E., Szabo, M. W., Neathery, T. L. & Copeland, C. W., Jr. 1988. Geologic Map of Alabama, northeast sheet. *Spec. Map Alabama geol. Surv.* **220**.

Passchier, C. W. & Simpson, C. 1986. Porphyroclast systems as kinematic indicators. *J. Struct. Geol.* **8**, 831–843.

Prouty, W. F. 1916. Preliminary report on the crystalline and other marbles of Alabama. *Bull. Alabama geol. Surv.* **18**.

Ramsay, D. M. 1979. Analysis of rotation of folds during progressive deformation. *Bull. geol. Soc. Am.* **90**, 732–738.

Ramsay, J. G. 1982. Rock ductility and its influence on the development of tectonic structures in mountain belts. In: *Mountain Building Processes* (edited by Hsü, K. J.). Academic Press, London, 111–127.

Rhodes, S. & Gayer, R. A. 1977. Non-cylindrical folds, linear structures in the X direction and mylonite developed during translation of the Caledonian Kalak Nappe Complex of Finmark. *Geol. Mag.* **114**, 329–341.

Rutter, E. H. 1974. The influence of temperature, strain rate and interstitial water in the experimental deformation of calcite rocks. *Tectonophysics* **22**, 311–334.

Schmid, S. M., Panozzo, R. & Bauer, S. 1987. Simple shear experiments on calcite rocks: rheology and microfabric. *J. Struct. Geol.* **9**, 747–778.

Shaw, C. E., Jr. 1970. Age and stratigraphic relations of the Talladega Slate: evidence of pre-middle Ordovician tectonism in central Alabama. *Southeast Geol.* **11**, 255–267.

Simpson, C. 1986. Determination of movement sense in mylonites. *J. Geol. Educ.* **34**, 246–261.

Simpson, C. & Schmid, S. M. 1983. An evaluation of criteria to deduce the sense of movement in sheared rocks. *Bull. geol. Soc. Am.* **94**, 1281–1288.

Skjernaa, L. 1989. Tubular folds and sheath folds: definitions and conceptual models for their development, with examples from the Grapesvare area, northern Sweden. *J. Struct. Geol.* **11**, 689–703.

Steltenpohl, M. G. 1989. Geology of the southernmost exposures of the Pine Mountain window, Alabama. In: *Southern Appalachian Windows* (Hatcher, R. D., Jr. & Thomas, W. A.). *Am. Geophys. Un. 21st Int. Geol. Congr. Field Trip Guidebook* **T167**, 21–28.

Steltenpohl, M. G. & Moore, W. B. 1988. Metamorphism in the Alabama Piedmont. *Alabama geol. Surv. Circ.* **138**.

Thomas, W. A. & Neathery, T. L. 1980. Tectonic framework of the Appalachian orogen in Alabama. In: *Excursions in Southeastern Geology* 2 (edited by Frey, R. W.). American Geological Institute, 465–526.

Tull, J. F. 1978. Structural development of the Alabama Piedmont northwest of the Brevard zone. *Am. J. Sci.* **278**, 442–460.

Tull, J. F. 1982. Stratigraphic framework of the Talladega slate belt, Alabama Appalachians. In: *Tectonic Studies in the Talladega and Carolina Slate Belts, Southern Appalachian Orogen* (edited by Bearce, D. N., Black, W. W., Kish, S. A. & Tull, J. F.). *Spec. Pap. geol. Soc. Am.* **191**, 3–18.

Tull, J. F. 1985. Stratigraphy of the Sylacauga Marble Group In: *Early Evolution of the Appalachian Miogeocline: Upper Precambrian–Lower Paleozoic Stratigraphy of the Talladega Slate Belt* (edited by Tull, J. F., Bearce, D. N. & Guthrie, G. M.). *Alabama geol. Soc. 22nd Ann. Field Trip Guidebook*, 21–26.

Tull, J. F. & Guthrie, G. M. 1985. Proposed stratigraphic linkages between the Talladega slate belt and the Appalachian miogeocline: tectonic implications. In: *Early Evolution of the Appalachian Miogeocline: Upper Precambrian–Lower Paleozoic Stratigraphy of the Talladega Slate Belt* (edited by Tull, J. F., Bearce, D. N. & Guthrie, G. M.) *Alabama geol. Soc. 22nd Ann. Field Trip Guidebook*, 1–10.

Tull, J. F., Harris, A. G., Repetski, J. E., McKinney, F. K., Garret, C. B. & Bearce, D. N. 1988. New paleontologic evidence constraining the age and paleotectonic setting of the Talladega slate belt, southern Appalachians. *Bull. geol. Soc. Am.* **100**, 1291–1299.

Vollmer, F. W. 1988. A computer model of sheath nappes formed during crustal shear in the Western Gneiss Region, central Norwegian Caledonides. *J. Struct. Geol.* **10**, 735–743.

Williams, G. D. 1978. Rotation of contemporary folds into the X direction during overthrust processes in Laksfjord, Finnmark. *Tectonophysics* **48**, 29–40.

APPENDIX

Combination of Skjernaa's (1989) *equations* (A3) *and* (A6)

Figure A1 illustrates geometric elements used for the combination of Skjernaa's (1989) equations (A3) and (A6). The resultant equation was used to create Fig. 11. The reader is referred Skjernaa (1989, appendix) for details of her calculations. The reader is also advised that simplifications have been made, as described by Skjernaa (1989), for cases of small α values.

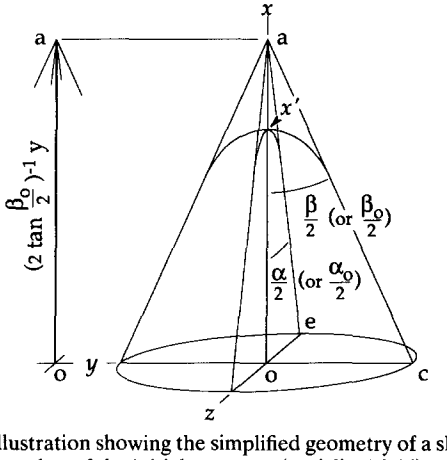

Fig. A1. Illustration showing the simplified geometry of a sheath fold or that of the initial structure (periclinal fold).

Referring to Fig. A1, simple trigonometric identities

$$\tan\frac{\alpha}{2}=\frac{oe}{oa} \quad \text{and} \quad \tan\frac{\beta}{2}=\frac{oc}{oa}$$

lead to the relations:

$$R_{zy}=\frac{oe}{oc}=\frac{\tan\frac{\alpha}{2}}{\tan\frac{\beta}{2}} \tag{A1}$$

and

$$R_{yz}=\frac{oc}{oe}=\frac{\tan\frac{\beta}{2}}{\tan\frac{\alpha}{2}}. \tag{A2}$$

Equation (A2) can be rearranged such that

$$\tan\frac{\beta}{2}=\tan\frac{\alpha}{2}R_{yz}. \tag{A3}$$

Combining equation (A3) and Skjernaa's (1989) equation (A6),

$$\tan\frac{\beta}{2}=\tan\frac{\beta_o}{2}\cos\tan^{-1}\gamma,$$

gives

$$\tan\frac{\alpha}{2}R_{yz}=\tan\frac{\beta_o}{2}\cos\tan^{-1}\gamma. \tag{A4}$$

This can be rearranged to give

$$\beta_o=2\tan^{-1}\left[\tan\frac{\alpha}{2}R_{yz}(\cos\tan^{-1}\gamma)^{-1}\right]. \tag{A5}$$

Finally, substituting Skjernaa's (1989) equation (A3),

$$\alpha=\left[\tan^{-1}\left(\gamma-\tan\frac{\alpha_o}{2}\right)^{-1}\right]-\left[\tan^{-1}\left(\tan\frac{\alpha_o}{2}+\gamma\right)^{-1}\right],$$

for α in equation (A5) gives

$$\beta_o=2\tan^{-1}\left[\tan\left(\frac{\left[\tan^{-1}\left(\gamma-\tan\frac{\alpha_o}{2}\right)^{-1}\right]-\left[\tan^{-1}\left(\tan\frac{\alpha_o}{2}+\gamma\right)^{-1}\right]}{2}\right)\cdot R_{yz}(\cos\tan^{-1}\gamma)^{-1}\right]. \tag{1}$$